

Multi-objective optimization for sustainable renewable jet fuel production: A case study of corn stover based supply chain system in Midwestern U.S.

Endai Huang^{a,1}, Xiaolei Zhang^{a,1}, Luis Rodriguez^b, Madhu Khanna^c, Sierk de Jong^d, K.C. Ting^b, Yibin Ying^{a,e}, Tao Lin^{a,*}

^a College of Biosystems Engineering and Food Science, Zhejiang University, Hangzhou, Zhejiang, China

^b Department of Agricultural and Biological Engineering, University of Illinois at Urbana-Champaign, Urbana, IL, USA

^c Department of Agricultural and Consumer Economics, University of Illinois at Urbana-Champaign, Urbana, IL, USA

^d Copernicus Institute of Sustainable Development, Faculty of Geosciences, Utrecht University, Utrecht, the Netherlands

^e Faculty of Agricultural and Food Science, Zhejiang A&F University, Hangzhou, Zhejiang, China

ARTICLE INFO

Keywords:

Renewable jet fuel
Supply chain optimization
Cost
Greenhouse gas emission
Pareto-optimal curve
Multi-objective optimization
Mixed-integer linear programming

ABSTRACT

Sustainable development of biomass-based renewable jet fuel (RJF) production mitigates the environmental stress and improves rural economics. We develop a mixed-integer linear programming model to incorporate spatial, agricultural, techno-economical, and environmental data for multi-objective optimization of RJF supply chain systems. The model is applied to the Midwestern U.S. to evaluate the sustainability performance of three pathways including alcohol-to-jet (ATJ), Fischer-Tropsch (FT) and Hydrothermal liquefaction (HTL). The results show that HTL is the most cost-effective with a cost of \$4.64/gal while FT is most environmental-friendly with the greenhouse gas (GHG) emissions of 0.10 kg CO₂/gal. The cost-optimal analysis suggests a centralized supply chain configuration with large facilities, while the environmental optimization analysis prefers a distributed system with small biorefinery facilities. For FT approach, cost optimization analysis suggests developing a supply chain with one large biorefinery, whereas environmental optimization prefers a system with 11 small biorefineries. Considering the economic and environmental factors simultaneously, the Pareto curve demonstrates that total production costs of three pathways all increase with the more stringent constraints of GHG emissions. This indicates that RJF production costs are sensitive to the regulation of GHG emissions. Considering the carbon price at \$0.22 per kg of CO₂ reduction, FT yields the lowest cost of \$2.83/gal among three pathways, but it is still 47% higher than that of fossil jet fuel. FT is not cost competitive with fossil jet fuel until the carbon price increases to \$0.30 per kg of CO₂ reduction. FT is suggested a promising sustainable RJF production pathway due to its relatively low capital investment and production costs, centralized supply chain configuration, and low GHG emissions.

1. Introduction

Aviation produces roughly 2% of the total carbon dioxide emissions globally [1]. The aviation industry will continue to grow due to the increasing transportation needs and there are no alternative to liquid fuels for aviation. The industry has committed to reducing its net carbon footprint by 2050 to below 50% of the amount in 2005 [2]. To achieve this goal, renewable jet fuel (RJF) production from a variety of biomass feedstocks is critical to reduce usage of fossil fuels and mitigate the environmental impact in the aviation sector [3–7]. Biomass-based RJF production reduces greenhouse gas (GHG) emissions and improves the diversity of energy resources [8–13].

Alcohol-to-jet (ATJ), Fischer-Tropsch (FT), and hydrothermal liquefaction (HTL) are three major technologies to convert biomass to jet fuel, certified or under review by American Society for Testing and Materials (ASTM) [14]. ATJ covers a wide range of technologies producing jet fuel from biomass via alcohol intermediates. Biomass is first converted to ethanol and further converted to a hydrocarbon fuel via dehydration, oligomerization, and hydrogenation [15]. FT is a biomass-to-liquids process that involves the gasification of biomass, Fischer-Tropsch synthesis, and catalytic cracking to produce synthetic paraffinic kerosene [16]. FT has been applied to fossil fuel feedstocks for several decades. HTL converts wet biomass to a bio-crude with a low oxygen content via thermal-catalytic conversion, where bio-crude is consequently upgraded

* Corresponding author.

E-mail address: lintao1@zju.edu.cn (T. Lin).

¹ E.H. and X.Z. contributed equally to this work.

Nomenclature		t_{f3}	unit fixed transportation cost between biorefineries and airports
<i>Decision variables of the optimization model</i>		e_b^i	unit biomass production GHG emissions in county i
Z_1	total annual RJF supply costs	e_s	unit CSP related GHG emissions
Z_2	total annual RJF supply GHG emissions	e_f	unit biorefinery related GHG emissions
C_B	biomass procurement costs	e_{t1}, e_{t2}, e_{t3}	unit transportation GHG emissions between four stages
C_S	CSP related costs	γ	biomass conversion rate from biomass to jet fuel
C_F	biorefinery related costs	a^m	jet fuel demand in airport m
C_T	biomass and jet fuel transportation related costs	ω	parameter for multi-objective optimization
E_B	biomass production GHG emissions	ε	parameter for ε -constraint method
E_S	CSP related GHG emissions	<i>Abbreviations</i>	
E_T	transportation related GHG emissions	ASTM	American Society for Testing and Materials
E_F	biorefinery related GHG emissions	ATJ	alcohol-to-jet
T_v	variable transportation costs	CAPEX	capital expenditures
T_f	fixed transportation costs	CSP	centralized storage and preprocessing
$f^{i,j}$	amount of biomass being transformed from county i to j	DSHC	direct sugars to hydrocarbons
p^j	total capacity in the CSP in county j	Ec	economic
q^k	total capacity in the biorefinery in county k	Env	environmental
<i>Parameters of the optimization model</i>		FT	Fischer-Tropsch
α	economic allocation factor	GHG	greenhouse gas
β	energy allocation factor	HEFA	hydroprocessed esters and fatty acids
$d^{i,j}$	distance between county i and j	HRJ	hydro-processed renewable jet
t_{v1}	unit variable transportation cost between supply sites and CSPs	HTL	hydrothermal liquefaction
t_{v2}	unit variable transportation cost between CSPs and biorefineries	LCA	life-cycle analysis
t_{v3}	unit variable transportation cost between biorefineries and airports	LP	linear programming
t_{f1}	unit fixed transportation cost between supply sites and CSPs	MASBI	Midwest Aviation Sustainable Biofuels Initiative
t_{f2}	unit fixed transportation cost between CSPs and biorefineries	MILP	mixed-integer linear programming
		MILFP	mixed-integer linear fractional programming
		OPEX	operational expenditure
		RJF	renewable jet fuel
		TEA	techno-economic analysis

using hydrogen [14]. Additionally, a few co-products including diesel and gasoline are generated in the process. Detailed descriptions of three conversion technologies can be found in Ref. [14].

Many studies have evaluated the feasibility of renewable fuel production by conducting techno-economic analysis (TEA) of various conversion technologies (Table 1). Among them, some studies provided

Table 1

Summary of various dimensions of previous studies on biomass supply chains. Ec = economic, Env = environmental; hydroprocessed esters and fatty acids, HEFA; direct sugars to hydrocarbons, DSHC; life-cycle analysis, LCA; techno-economic analysis, TEA; mixed-integer linear programming, MILP; linear programming, LP; mixed-integer linear fractional programming, MILFP.

Purpose	Objective	Pathway (Region)	Year	Method	Object	Reference
Technological Dimension	Ec	Hydro-processed renewable jet	2016	TEA	RJF	[17]
	Ec	HEFA, FT, HTL, ATJ, and DSHC	2015	TEA	RJF	[14]
	Ec	Hydrolysis, decarboxylation, and reforming	2015	TEA	RJF	[18]
	Ec	HEFA	2013	TEA	RJF	[19]
	Ec	MixAlco process	2010	TEA	Gasoline, jet fuel, and diesel	[20]
	Env	HEFA, FT, HTL, ATJ, DSHC, and pyrolysis	2017	LCA	RJF	[25]
	Env	Hydrotreating/Hydrocracking based conversion, gasification, and FT-Synthesis	2011	LCA	Biojet	[24]
	Ec + Env	Sugars fermentation	2017	TEA and LCA	RJF	[26]
	Ec + Env	Pyrolysis	2017	TEA and LCA	Electricity, heat, and char	[27]
	Ec + Env	HEFA	2014	TEA and LCA	Hydroprocessed jet and diesel fuel	[28]
Supply Chain Dimension	Ec	California (County)	2018	MILP	Renewable diesel and biojet fuel	[40]
	Ec	Sweden (Sector)	2017	MILP	Diesel, gasoline and light ends	[25]
	Ec	Illinois (County)	2014	MILFP	Gasoline, diesel and jet fuel	[41]
	Ec	Illinois (County)	2013	MILP	Ethanol	[38]
	Ec	United States (County)	2013	MILP	Gasoline, diesel, and jet fuel	[42]
	Env	Michigan (County)	2013	LP + LCA	Bioethanol	[43]
	Ec + Env	Kansas (Grid)	2014	MILP	Ethanol	[44]
	Ec + Env	Illinois (County)	2013	MILFP + LCA	Gasoline and diesel	[45]
	Ec + Env	Iowa (County)	2011	MILP + LCA	Liquid transportation fuel	[46]

detailed analyses for individual technology, such as hydro-processed renewable jet (HRJ) process [17], hydroprocessed esters and fatty acids (HEFA) process [19], and MisAlco process [20]. A comprehensive TEA compared five conversion technologies, including HEFA, ATJ, FT, HTL, and direct sugars to hydrocarbons (DSHC) for economic performance [14]. Several studies evaluated the economic performance of RJF production from various biomass feedstocks, including jatropha, camelina oil, soybean oil, lignocelluloses, microalgae oil, nut shell liquid, and others [17–22]. Minimum jet fuel selling price was estimated to be \$5.42/gal for HRJ [17]. The production cost for ATJ, FT, and HTL was estimated to range between \$9.18–13.76/gal, \$6.71–9.71/gal, and \$3.71–5.12/gal, respectively [14]. These production costs are much higher than the market price of jet fuel of \$1.93/gal [14,23].

To estimate the environmental impact of alternative fuels, life-cycle analysis (LCA) has been applied to estimate GHG emissions intensity of RJF and compare it to fossil jet fuel [24]. The results showed that several conversion pathways, such as FT, HTL, and ATJ pathways, can reduce GHG emissions intensity by 86–104%, 77–80%, and 60–75%, respectively, as compared to fossil jet fuel [25]. Some studies integrated TEA and LCA to evaluate the economic and environmental performance [26–28]. However, most LCA and TEA studies focus on conversion technologies, without much consideration of the complexity of the supply chain system and spatial characteristics of biomass production and transportations.

Renewable energy production requires systems analysis as a result of distributed biomass resources and low energy density of raw biomass [29,30]. Geographically, biomass supply sites and airports are not necessarily contiguous [31]. As a result of low energy density and dispersed nature of biomass, a biomass supply chain system requires a large sourcing region to meet a given demand for economic benefits [32–35]. Establishing a bioenergy industry requires consideration of many factors such as feedstock availability, conversion technology, and facility locations [25,36,37]. To handle these problems, strategic optimization of biomass supply chain is critical to optimize the numbers, locations, and capacities of facilities at each stage of supply chain and biomass flow patterns between these stages.

Many studies have been reported on economic optimization of biomass supply chain systems. A three-stage supply chain model including feedstock supply sites, centralized storage and preprocessing (CSP) sites and biorefineries was developed to minimize ethanol production costs [38]. The optimal mix of four strategies, scale, integration, transportation and supply chain configurations, was to minimize costs has also been evaluated [25]. Financial incentives and limited availability of biomass feedstocks are considered in a biofuel supply chain GeoSpatial and

Temporal Optimizer [40]. Existing energy infrastructure was also incorporated in systems analysis to save the capital and transportation costs in a hydrocarbon biofuel supply chain [41]. A biomass-to-liquid system optimization framework was proposed to quantify the impact of various fuel product ratios of gasoline, diesel and jet fuel [42]. Most of these studies leverage mixed integer programming as a model framework and consider spatial characteristics of biomass availability and transportation networks for economic optimization [25,38–42]. However, these studies typically do not consider the material flows between biorefinery and end-use fuel consumption like the airport. Airports are often located in metropolitan cities, which might be far away from biomass supply regions. The complete system design should consider the spatial mismatch between feedstock supply and end use.

Environmental performance has also been considered in supply chain analysis for ethanol production [43]. Economic revenue was maximized from positive environmental impacts in a multi-objective model for bioethanol production [44]. LCA was incorporated in mixed-integer nonlinear programming algorithms to measures both the economic and environmental performances for gasoline and diesel production [45]. A supply chain optimization model was designed under economic and environmental criteria and solved with the ϵ -constraint method [46]. Most supply chain optimization studies focus on single objective optimization and do not conduct multi-objective supply chain optimization which limits their potential to analyze trade-offs between economic and environmental sustainability. To the best of our knowledge, no previous research has applied multi-objective supply chain optimization for RJF production. The development of biomass-based renewable fuel production is highly affected by the supply chain configuration, as a result of spatial heterogenous feature of biomass availability and transportation system. There exists a critical gap to evaluate the sustainability performance of various RJF production technologies with the consideration of both economic and environmental performance under an optimal supply chain configuration.

The objectives of this study are to (1) develop a multi-objective optimization model to optimize regional biomass-based renewable jet fuel supply chain configurations by considering both economic and environmental impacts; (2) quantify the optimal supply chain configurations for three RJF conversion pathways by conflating spatial, agricultural, and economic inputs and constraints; and (3) identify an optimal renewable jet fuel pathway by considering the trade-offs between economic and environmental impacts using Pareto analysis.

The rest of this article is organized as follows. In Section 2, a detailed formulation of the multi-objective supply chain optimization

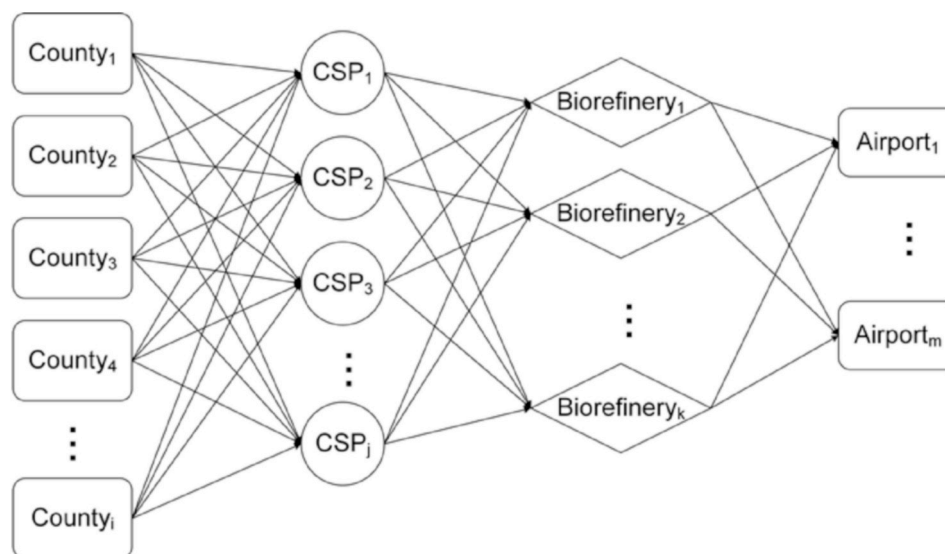


Fig. 1. A four-stage supply chain optimization model for renewable jet fuel production.

model is presented with the introduction of three conversion pathways of biomass based jet fuel production. Section 3 presents a scenario description of the biomass based jet fuel supply chain system in the Midwest Aviation Sustainable Biofuels Initiative (MASBI) region. Section 4 presents detailed results and discussions on the supply chain configurations under economic and environmental optimization as well as the Pareto-optimal curve for sustainability evaluation. The concluding remarks are summarized in Section 5.

2. Methods

2.1. Supply chain model description

The model used in this study is modified from the BioScope optimization model [38], which was originally designed for a three-stage biomass-to-ethanol supply chain (farms, centralized storage and preprocessing (CSP) sites, and biorefineries). The model is extended here to consider a four-stage biomass-to-renewable jet fuel supply chain, including biomass supply counties, CSPs, biorefineries, and airports (Fig. 1). Comparing to the original BioScope economic optimization model, the revised model focuses on the systems optimization of sustainability evaluation with multi-objective analysis. Both economic and environmental performance and constraints have been incorporated in the analysis. The key updates include the costs for renewable jet fuel production, GHG emissions for all supply chain sectors, jet fuel transportation, and jet fuel demands at airports.

The economic objective of the optimization model is to minimize the total annual RJF supply costs (Z_1) which are comprised of four parts: biomass procurement costs (C_B), biomass and jet fuel transportation related costs (C_T), CSP related costs (C_S), and biorefinery related costs (C_F) (Eq. (1)). α is an economic allocation factor for RJF as co-products are produced during the RJF production.

$$\text{Minimize } Z_1 = \alpha(C_B + C_S + C_F) + C_T \quad (1)$$

Transportation related costs (C_T) include variable transportation (T_v) and fixed transportation costs (T_f). The transportation costs of raw and preprocessed biomass are allocated among different co-products (Table 2) by the allocation factor α . In addition, T_v and T_f in Bioscope model can be modified by adding new variables to account for the jet fuel distribution costs for this four-stage model as shown in Eqs. (2) and (3). The variable jet fuel distribution cost is a function of unit variable transportation cost (t_{v3}), amount of biomass being transformed ($f^{k,m}$) and the transportation distance ($d^{k,m}$). Fixed jet fuel distribution cost depends on unit fixed transportation cost (t_{f3}) and the amount of renewable jet fuel being transported ($f^{k,m}$).

$$T_v = \alpha \sum_i \sum_j (t_{v1} \times f^{i,j} \times d^{i,j}) + \alpha \sum_j \sum_k (t_{v2} \times f^{j,k} \times d^{j,k}) + \sum_k \sum_m (t_{v3} \times f^{k,m} \times d^{k,m}) \quad (2)$$

$$T_f = \alpha \sum_i \sum_j (t_{f1} \times f^{i,j}) + \alpha \sum_j \sum_k (t_{f2} \times f^{j,k}) + \sum_k \sum_m (t_{f3} \times f^{k,m}) \quad (3)$$

As the model extends RJF distribution to airports, new airport-related constraints, such as the demand for fuel at the airport, must be added. Considering the mass balance, the jet fuel production in biorefinery k is equal to the total amount of jet fuel transported from biorefinery k to airport m ($f^{k,m}$) (Eq. (4)).

$$\sum_m f^{k,m} = q^k \times \gamma \quad (4)$$

where q^k is the total capacity in the biorefinery in county k , and the γ is biomass conversion rate from biomass to jet fuel. Similarly, the total amount of jet fuel transported to airport m should equal the demand at airport m (a^m) (Eq. (5)).

$$\sum_k f^{k,m} = a^m \quad (5)$$

Environmental performance is measured by GHG emissions including CO_2 , CH_4 , and N_2O , which are grouped together into a single indicator in terms of carbon dioxide equivalent emissions (CO_2 -equiv) based on 100-year global warming potential [25]. The environmental objective of the model is to minimize the total GHG emissions (Z_2) that comprises biomass production GHG emissions (E_B), transportation related GHG emissions (E_T), CSP related GHG emissions (E_S), biorefinery related GHG emissions (E_F) as shown in Eq. (6). β is an energy allocation factor due to co-products generated in RJF production.

$$\text{Minimize } Z_2 = \beta(E_B + E_S + E_F) + E_T \quad (6)$$

Biomass production related GHG emissions (E_B) are a function of optimal biomass flow ($f^{i,j}$) from supply sites to CSP sites and the county-level unit biomass production GHG emissions (e_b^i) as shown in Eq. (7). In the current study, we assume that unit CSP related GHG emissions (e_{csp}) and unit biorefinery related GHG emissions (e_f) are constant regardless of the capacity. Therefore, total CSP and biorefinery related GHG emissions are linearly dependent on total capacities (Eqs. (8) and (9)). GHG emissions in transportation between each stage make up total transportation GHG emissions (E_T). Transportation related GHG emissions are a function of unit GHG emissions at each stage (e_{t1} , e_{t2} , e_{t3}), amount of biomass being transported ($f^{i,j}$, $f^{j,k}$, $f^{k,m}$), and the transportation distance ($d^{i,j}$, $d^{j,k}$, $d^{k,m}$) (Eq. (10)). Given that multiple products produced in HTL and ATJ processes, the GHG emissions of moving raw and preprocessed biomass are also allocated among different co-products (Table 2).

$$E_B = \sum_i \sum_j e_b^i \times f^{i,j} \quad (7)$$

$$E_S = \sum_j e_s \times p^j \quad (8)$$

$$E_F = \sum_k e_f \times q^k \quad (9)$$

$$E_T = \beta \sum_i \sum_j e_{t1} \times f^{i,j} \times d^{i,j} + \beta \sum_j \sum_k e_{t2} \times f^{j,k} \times d^{j,k} + \sum_k \sum_m e_{t3} \times f^{k,m} \times d^{k,m} \quad (10)$$

The inputs of the model can be categorized into spatial, agricultural, techno-economical, and environmental perspectives (Fig. 2). Spatial information includes candidate counties for biomass production supply sites, CSPs, biorefinery facilities, and airport locations, as well as distance among these locations. The road network data is extracted from the existing road network, and the distance between candidates are calculated through ArcGIS. Agricultural related data includes biomass planted area, biomass yield and production cost in each supply county. Techno-economic inputs include unit biomass transportation costs before and after preprocessing, RJF transportation costs, as well as capital and operating costs for preprocessing and biorefinery. Environmental information includes GHG emissions for biomass production,

Table 2
Co-products and conversion rate for three technologies.

Product	Unit price (\$/Mg) [14]	Conversion rate (Mg/Mg corn stover)		
		ATJ	FT	HTL
Jet fuel	637.45	0.12	0.18	0.02
Diesel	592.30	0.01	0	0.07
Gasoline	557.77	0	0	0.11
Naphtha	482.07	0.026	0	0
Heavy fuel oil	613.55	0	0	0.04
Total biofuel yield		0.16	0.18	0.23

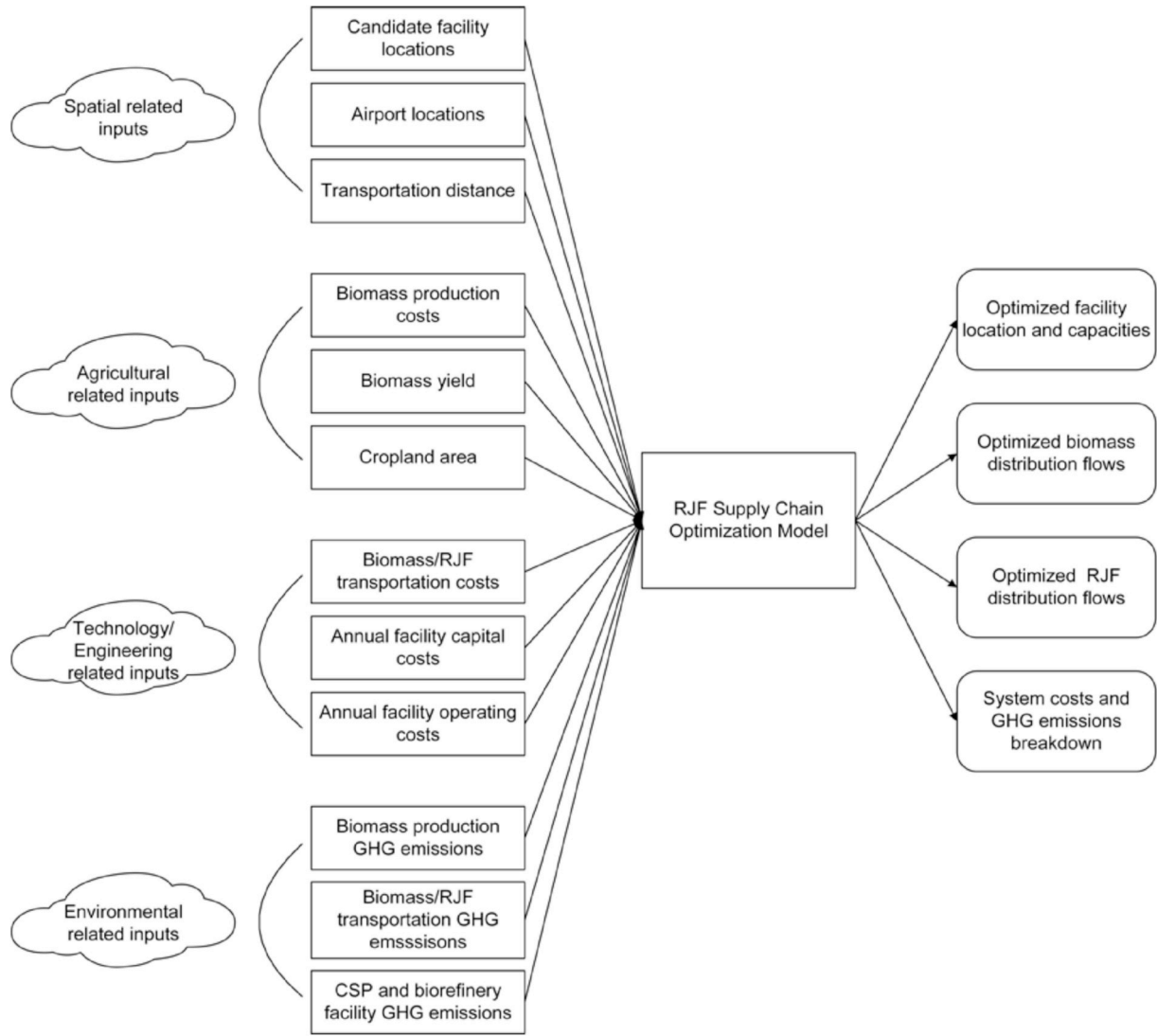


Fig. 2. Input and output of the RJF supply chain optimization model.

Table 3

The economic and energy allocation factors of RJF for three conversion pathways.

Factor	ATJ	FT	HTL
Economic allocation	0.79	1	0.11
Energy allocation	0.75	1	0.10

Table 4

The estimated jet fuel demand of the top five airports in the MASBI region [52].

Airport	State	Jet fuel demand in 2014 (Million gallons/yr)	Estimated RJF demand (Million gallons/yr)
ORD	IL	1,006.5	50.3
DTW	MI	312.2	15.6
CVG	KY	147.4	7.4
MDW	IL	134.7	6.7
IND	IN	130	6.5
Total		1,730.8	86.5

transportation, CSP and biorefinery production. For the transportation GHG emissions within the county, we assume that the transportation distance within the county is 2/3 of the radius of that county, which is calculated by the area of each county.

The decision variables include the optimal number, location, and capacity of biomass supply sites, CSPs, and biorefineries, as well as the optimal biomass and jet fuel flow patterns between each stage. The optimization model is a mixed integer linear programming model with the optimality gap set at 1%. The model is developed on Python platform and solved through Gurobi 7.0.

2.2. Multi-objective optimization

An ε -constraint method is used to solve the multi-objective optimization, which optimizes economic objective by restricting the environmental objective under a user-specified range [46]. The first step is to determine the range of GHG emissions based on the following equations:

The upper bound is obtained by minimizing Eq. (11),

$$\text{minimize: } \omega \cdot Z_1 + Z_2 \quad (11)$$

The lower bound is acquired by minimizing Eq. (12),

$$\text{minimize: } Z_1 + \omega \cdot Z_2 \quad (12)$$

where Z_1 and Z_2 represent the total production costs and total GHG emissions respectively, and ω is a very small value (on the order of 10^{-7}). The range between the upper and lower bound is divided into 19 identical intervals (20 break points). The total annual RJF production cost (Z_1) is minimized under the additional constraint that the total

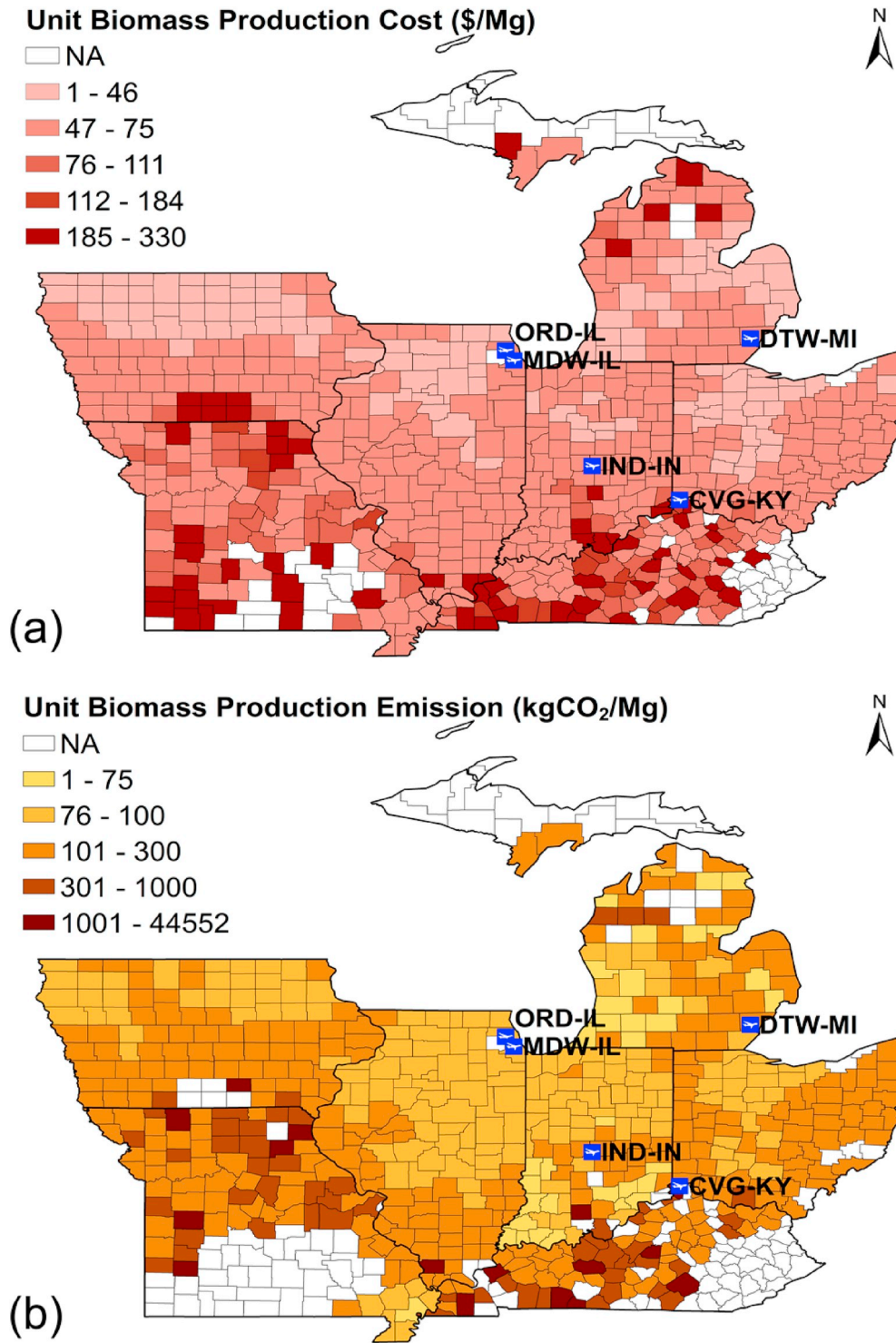


Fig. 3. Spatial visualization of the county-level biomass production costs (a) and GHG emissions (b).

GHG emissions should not exceed the level of break point ε for each scenario (Eq. (13)). An approximated Pareto-optimal curve is then generated for each conversion technology, which is used to evaluate the sustainability performance of renewable jet fuel production.

$$\begin{aligned} & \text{minimize: } Z_1 \\ & \text{s. t. : } Z_2 \leq \varepsilon \end{aligned} \quad (13)$$

The Pareto-optimal curve of different RJF pathways would vary in cost and GHG emissions. To compare different technologies with conventional jet fuel production, the monetization of CO₂ is used to provide

credits to three RJF pathways for the saving of GHG emissions. The conventional jet fuel production cost of \$1.93/gal [14] with a GHG emission at 11.67 kg CO₂/gal [25] is used as a baseline. According to a previous study, one additional kg of CO₂ emissions would introduce an additional social cost by \$0.22 [47]. The Pareto-optimal curves are shifted by monetizing the savings of GHG emissions with the above social cost.

2.3. Biorefinery conversion pathways

ATJ, FT, and HTL are three technologies to convert biomass to jet fuel.

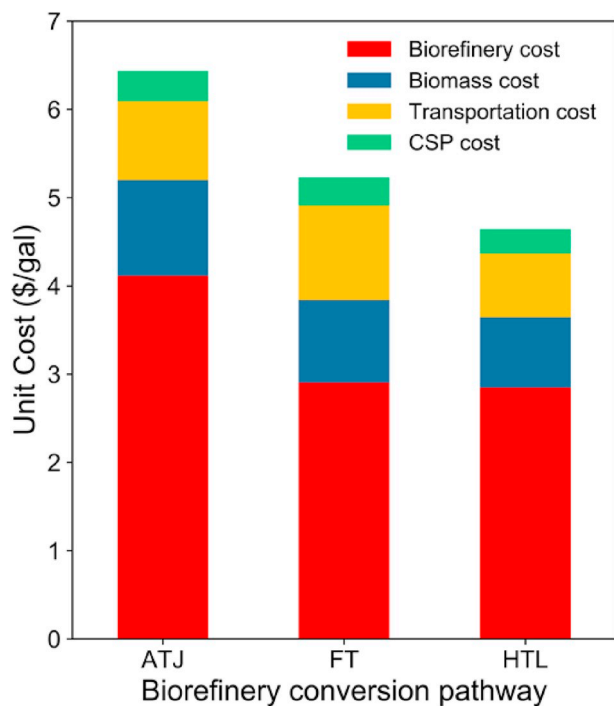


Fig. 4. Breakdown of the minimum production costs for three conversion pathways under cost optimization.

Table 5

Quantity and capacity range of the supply counties, CSPs, and biorefineries in the scenario of economic optimization analysis. All three pathways are optimized to meet the same level of total jet fuel demand.

	Supply County		CSP		Biorefinery	
	Number	Supply range (1000 Mg)	Number	Capacity range (1000 Mg)	Number	Capacity range (1000 Mg)
ATJ	9	62–862	7	210–862	2	377–1,772
FT	6	8–862	2	862–952	1	1,465
HTL	49	2–998	31	100–1,531	6	1,752–2,000

FT is used only for RJF production and has the highest biomass-to-RJF conversion rate. For HTL and ATJ processes, co-products such as diesel, gasoline, naphtha, and heavy fuel oil are generated. Electricity is generated during the jet fuel production process for three conversion technologies. The biomass-to-RJF conversion rate for ATJ, FT, and HTL are 0.12, 0.18, and 0.02 Mg jet fuel per Mg corn stover [14]. Detailed descriptions of the technologies have been reported for ATJ [48,49], FT [49], and HTL [50].

The biorefinery related costs are divided into capital expenditures (CAPEX), operational expenditure (OPEX), and CAPEX-dependent OPEX. The economies of scale effect is considered in capital related costs. A piecewise linear approximation is applied to linearize the cost curve into three capacity levels [38], namely small (50,000–600,000 Mg/yr), medium (600,000–1,300,000 Mg/yr), and large (1,300,000–2,000,000 Mg/yr) biomass input scales for CAPEX estimation. A scaling factor of 0.7 and an annuity factor of 0.121 are used for biorefinery cost estimation (Fig. A.1 and Table A.1). The OPEX includes utilities and other raw materials as well as the electricity credit (Table A.2). The total OPEX for three conversion technologies are \$56, 10, and 43 per Mg corn stover. CAPEX-dependent OPEX is calculated from the CAPEX using a factor of 0.105 [51].

The biorefinery related GHG emissions are proportional to the quantity of jet fuel production. We use the displacement method [25] for electricity generated during the jet fuel production process. The GHG emissions for ATJ, FT, and HTL pathways are 0.85, -1.30, and

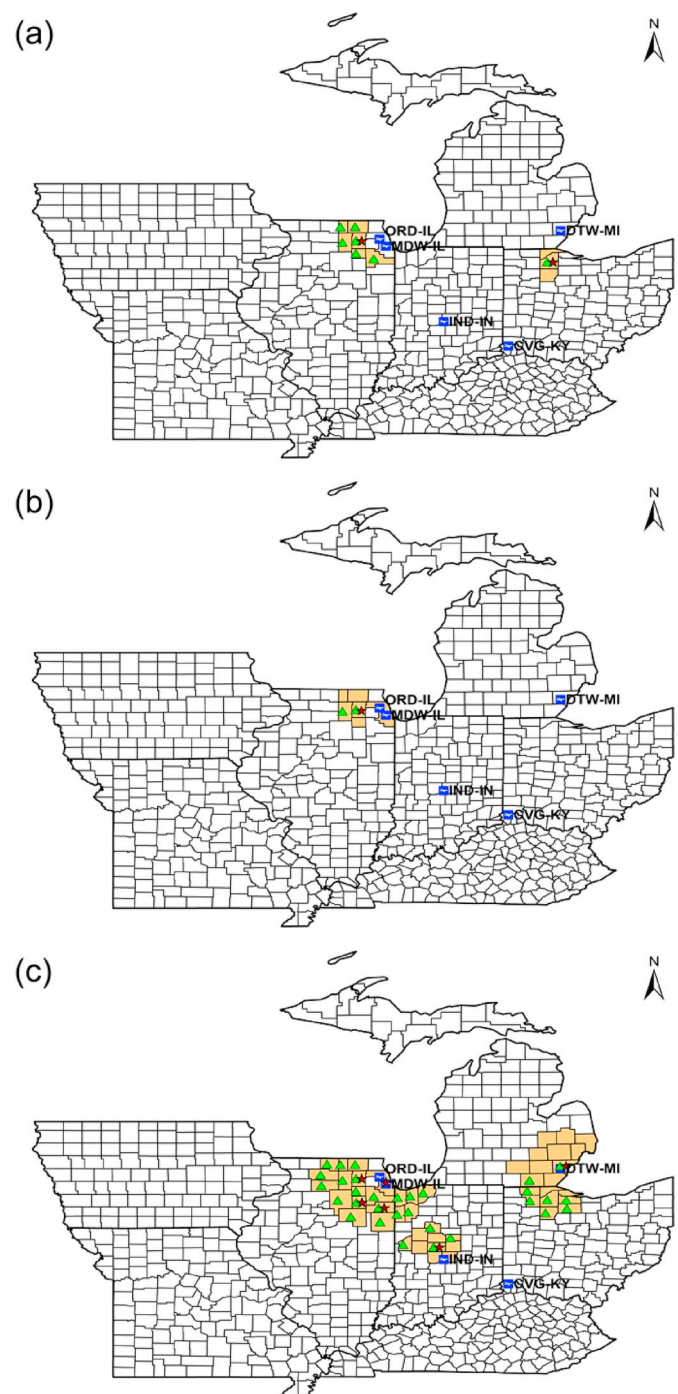


Fig. 5. Optimal supply chain configurations under economic optimization: (a) ATJ; (b) FT; (c) HTL. Colored areas represent selected biomass supply counties, triangles represent CSP facilities, and stars represent biorefineries.

2.01 kg CO₂/gal, respectively. The negative value for FT is due to the electricity generated during the jet fuel production that offsets the GHG emissions (Table A.3).

Due to the co-products generated in the production (Table 2), we use allocation methods to estimate the real value of the cost and GHG emissions from jet fuel production. Allocation methods are based on the physical properties of the co-products and less susceptible to method choice and uncertainties [25]. For the cost analysis, the economic allocation that allocates the total production costs by the mass and unit price of co-products is used. Thus, fuel co-product value can be incorporated in the RJF production. For the GHG emission analysis, we

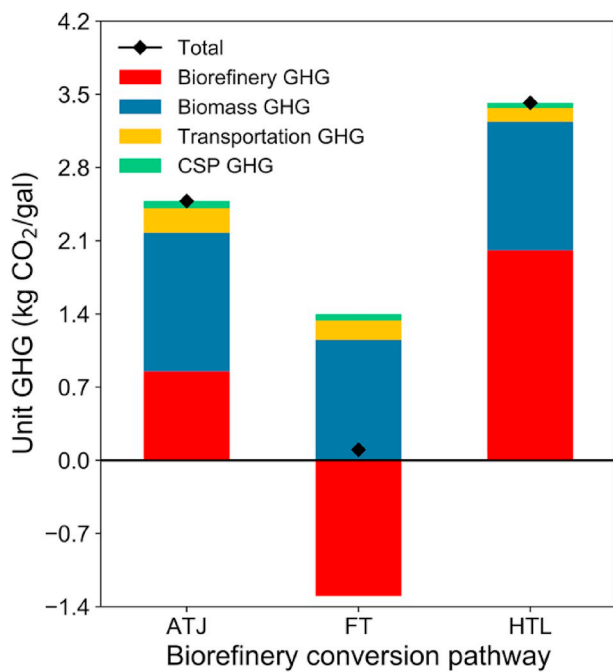


Fig. 6. Breakdown of the GHG emissions for three conversion pathways under environmental optimization.

use energy allocation which allocates the total GHG emissions by the share of energy of each co-products except for electricity. The economic and energy allocation factors for each pathway are presented in Table 3.

3. Scenario description

We apply the modified BioScope model in the Midwest Aviation Sustainable Biofuels Initiative (MASBI) region of the U.S. as a case study. MASBI region consists of 699 counties from seven states, including Illinois (IL), Iowa (IA), Indiana (IN), Missouri (MO), Kentucky (KY), Ohio (OH), and Michigan (MI). The five largest airports in MASBI region are O'Hare International Airport (ORD), Detroit Metropolitan International Airport (DTW), Cincinnati/Northern Kentucky International Airport (CVG), Midway International Airport (MDW), and Indianapolis International Airport (IND), each with an annual demand greater than 100 million gallons (Table 4). In this paper, we analyze the implications of replacing five percent of jet fuel demand in each airport with renewable jet fuel, which is a total demand of 86.5 million gallons annually. Each county in the MASBI region is considered as a candidate site of biomass supply, CSP, and biorefinery.

We implement and compare three conversion pathways of ATJ, FT and HTL to satisfy the above jet fuel demand in MASBI region. The amount of corn stover that can be harvested from each county depends on the yield of corn and the no-tillage practice used. With no-till practice, 50% of the stover can be harvested without adverse effects on soil fertility. Agricultural data includes county-level biomass planted area [53], biomass yield, biomass production cost (Fig. 3a), and unit GHG emission of biomass production (Fig. 3b). Transportation and CSP related costs and GHG emissions are based on previous studies, such as unit biomass transportation cost before and after preprocessing [38,39], unit jet fuel transportation cost [46], unit CSP operating emission [54], and unit transportation GHG emission [25]. Detailed information is provided in Tables A.4–A.7.

4. Results and discussion

4.1. Supply chain analysis under economic optimization

The results of economic optimization show that HTL yields the lowest production cost at \$4.64/gal, while ATJ and FT require a higher

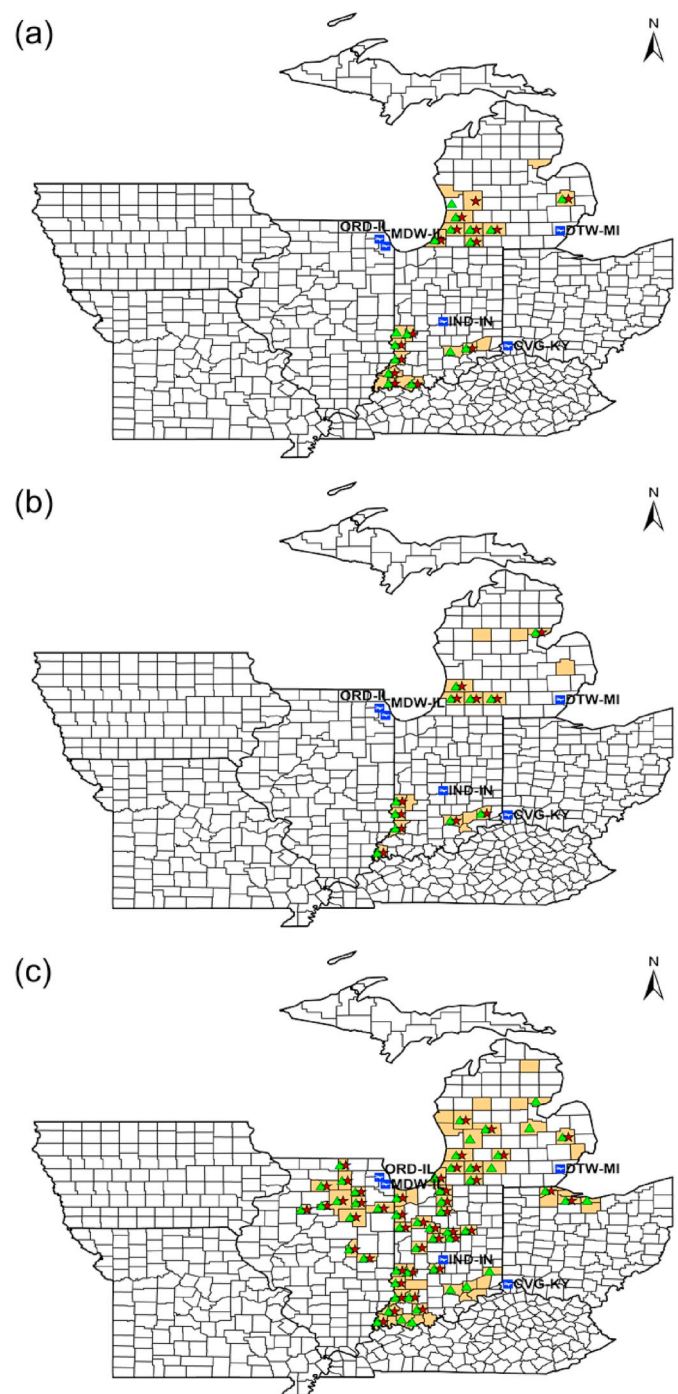


Fig. 7. Optimal supply chain configurations under environmental optimization: (a) ATJ; (b) FT; (c) HTL. Colored areas represent selected biomass supply counties, triangles represent CSP facilities, and stars represent biorefineries.

Table 6

Quantity and capacity range of the supply counties, CSPs, and biorefineries in the scenario of environmental optimization.

	Supply County		CSP		Biorefinery	
	Number	Supply range (1000 Mg)	Number	Capacity range (1000 Mg)	Number	Capacity range (1000 Mg)
ATJ	22	35–270	17	101–270	15	100–218
FT	17	16–270	11	122–270	11	100–218
HTL	71	0.2–936	55	100–936	45	100–600

Table 7
Unit production costs and GHG emissions under economic and environmental optimization.

	Economic optimization		Environmental optimization	
	Cost (\$/gal)	GHG emissions (kg CO ₂ /gal)	Cost (\$/gal)	GHG emissions (kg CO ₂ /gal)
ATJ	6.43	3.12	9.67	2.48
FT	5.23	0.76	8.33	0.10
HTL	4.64	3.65	6.45	3.42

cost of \$6.43 and \$5.23/gal, respectively (Fig. 4). Three conversion technologies demonstrate a similar pattern in cost allocation. Biorefinery related costs are the most significant components, followed by the biomass procurement, transportation, and CSP related costs. Biorefinery related costs account for 64.0%, 55.6%, and 61.4% of the total cost for ATJ, FT, and HTL, respectively. The optimal systems, therefore, choose to develop large-scale biorefineries to achieve the economy of scales for production cost reduction (Table 5). Although the jet fuel demand is fixed for the analysis, the required biomass supply varies as a result of differences in conversion rate by three approaches. The investment of CSP and biorefinery facilities for HTL is 8.65 billion dollars, which is significantly higher than ATJ and FT with 1.59 and 1.12 billion dollars, respectively (Table A.8). The high capital investment cost by HTL is mainly a result of its increased number of biorefineries. HTL approach requires six large biorefinery facilities, as compared to one and two biorefineries for FT and ATJ, respectively (Table 5). HTL approach provides a lowest biomass-to-RJF conversion rate due to several co-products (Table 2), thus it requires significantly large scale to meet the same jet fuel demand compared with other two approaches. HTL has the highest biofuel yield rate with a variety of valued co-products such as heavy fuel oil and diesel (Table 2), which drives down its unit production costs for jet fuel.

Cost-optimal supply chain analyses suggest a centralized configuration for all three pathways (Fig. 5). Large-scale centralized facilities are selected to take advantage of the economies of scale to reduce the biorefinery related cost. The locations of all selected biorefinery facilities among three approaches are located near major airports, especially for the largest airport in Chicago; even when the system is designed to satisfy 5% of jet fuel demand at each airport (Fig. 5). All three approaches choose counties in northern Illinois as major biomass supply regions (Fig. 5), due to its low procurement costs and reduced transportation costs. Different technologies, however, require different supply chain configurations in terms of the number of supply counties and facilities, as a result of differences in the biomass to jet fuel

conversion rate and biorefinery costs. HTL approach requires the largest biomass sourcing area (49 supply counties and 31 CSP facilities) to support biorefinery productions. ATJ and FT approaches require only nine and six counties as biomass supply sites to meet the demand, which are mainly located in northern Illinois (Fig. 5). The selected supply chain configuration for FT approach is located on the west of all airports, which demonstrates that the system is more sensitive to the changes of biomass procurement and transportation costs, as compared to the jet fuel transportation costs. The low biomass procurement costs in northern Illinois (Fig. 3) drives the optimal design of RJF supply chain configuration to be located in the west of airports, instead to be located in the middle of these airports for the minimization of jet fuel transportation distance.

4.2. Supply chain analysis under environmental optimization

FT is the most environmental-friendly pathway with a GHG emission of 0.10 kg CO₂/gal, followed by the ATJ of 2.48 kg CO₂/gal and HTL of 3.42 kg CO₂/gal under environmental optimization (Fig. 6). Biomass production accounts for the significant proportion of GHG emissions for three pathways, while transportation and CSP related GHG emissions only represent a very small fraction. Counties with low biomass production GHG emissions are, therefore, selected for biomass related GHG emissions reduction. A large number of CSPs are planned to preprocess biomass locally to reduce transportation related GHG emissions. Biorefinery related GHG emissions vary as a result of the impact of co-products production. FT shows a negative net biorefinery related GHG emissions, largely due to the amount of electricity generated during the jet fuel production. This is consistent with a previous study that shows negative GHG emissions due to co-product credits [25]. HTL and ATJ approaches generate positive GHG emissions. In particular, biorefinery related GHG emissions account for the largest component for HTL. Three approaches have varied unit GHG emissions for biomass production and transportation, as a result of their different optimal supply chain configurations such as facility numbers and locations.

For the minimization of GHG emissions, the optimal supply chain configurations show a distributed pattern for three conversion pathways (Fig. 7). The optimal systems consist of a large number of small facilities, aiming for the localized production (Table 6). The largest biorefinery capacity among three technologies is below 0.6 million Mg per year of biomass input. This is very different compared to centralized production under the cost optimization scenario.

The optimal systems choose the supply counties with low unit biomass production GHG emissions (Figs. 3b and 7). ATJ and FT approaches choose counties in southwest Indiana and southern Michigan as major biomass

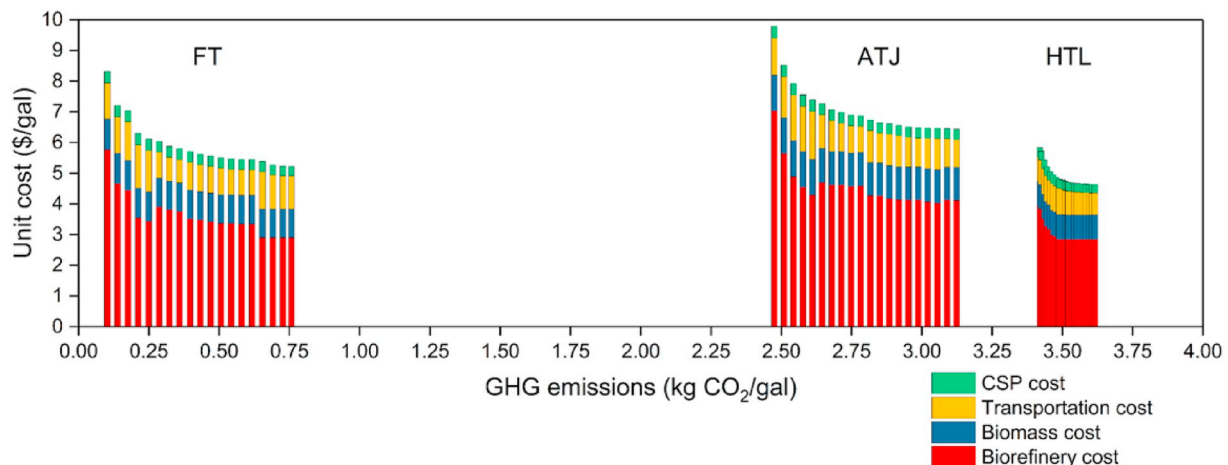


Fig. 8. Pareto-optimal curves for three RJF pathways. Each pathway has been analyzed under 20 GHG emissions levels. FT is within 0.10–0.76 kg CO₂/gal; ATJ is within 2.48–3.12 kg CO₂/gal; HTL is within 3.42–3.62 kg CO₂/gal.

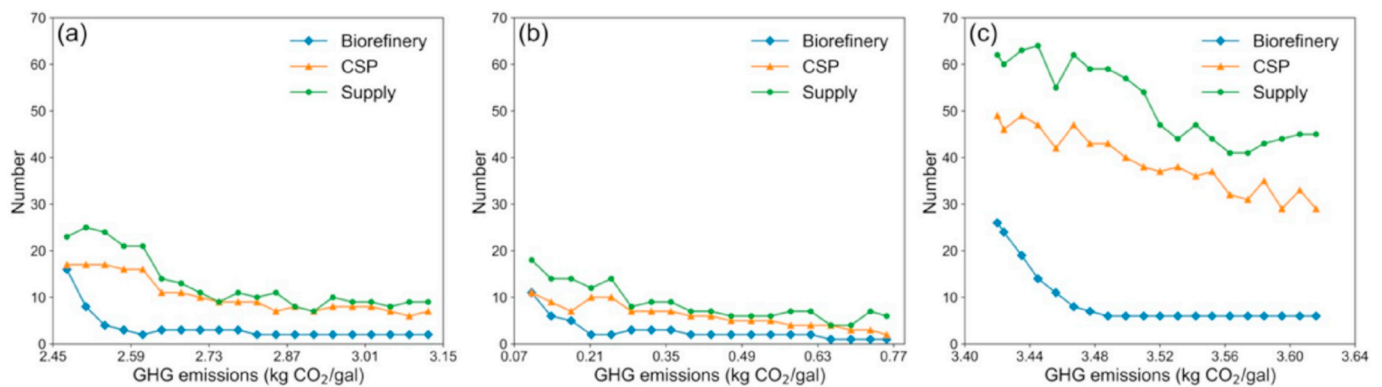


Fig. 9. Number of supply counties, CSPs, and biorefineries under Pareto-optimal curve analysis: (a) ATJ; (b) FT; (c) HTL.

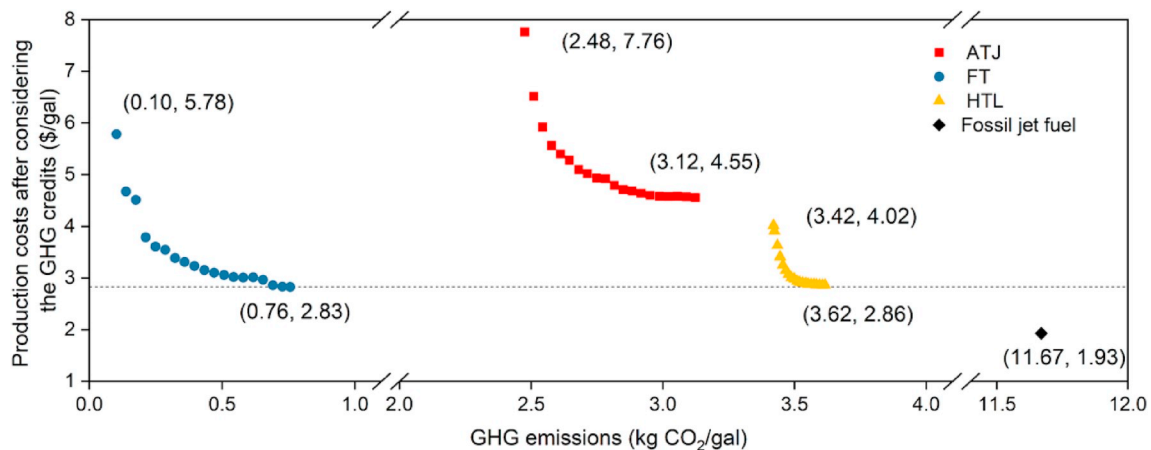


Fig. 10. Pareto-optimal curve for three conversion pathways after considering the credit of GHG emissions. A black diamond represents the performance of fossil jet fuel production.

sourcing regions due to its relatively low unit GHG emissions of biomass production. For HTL, the major supply counties are located in northern Illinois, because of the large biomass supply and relatively low production and transportation emissions. A large number of CSP and biorefinery facilities are constructed near the biomass supply counties for local processing (Fig. 7). Although such a distributed configuration leads to a rise in jet fuel transportation related GHG emissions, the decline of GHG emissions in biomass production overweighs the increase in transportation. Biomass production GHG emissions are more significant, about 7–10 times than transportation related emissions. In most cases, the CSP and biorefinery facilities are built in the same supply county. There is no scale effect for CSP and biorefinery related GHG emissions and hence no benefit to building large-scale CSPs or biorefineries. This location decision can reduce the biomass transportation distance and the transportation related GHG emissions. The number of supply counties, CSPs and biorefineries for HTL is much larger than the other two conversion ways, because of its low jet fuel yield rate. Among three pathway scenarios, southern Indiana and southwest Michigan are selected as the common supply regions.

4.3. Comparison of economic and environmental optimizations

The cost-optimal analysis suggests a centralized supply chain configuration with large facilities; whereas the environmental optimization analysis prefers a distributed biomass supply chain with many CSP and biorefinery facilities (Figs. 5 and 7). Since biorefinery related costs are a major contribution for total costs, the cost-optimal supply chain suggests to develop a few but large-scale biorefinery facilities (0.4–2 million Mg) to take advantage of economies of scale to reduce the biorefinery related cost (Table 5). For GHG-optimal scenario, widespread small biorefineries

(0.1–0.6 million Mg) are built near the supply counties and CSPs (Table 6). Since biomass production accounts for the major GHG emissions, the system suggests to develop small facilities near counties with low GHG emissions of biomass production. The selected supply regions for GHG minimization, therefore, are much larger than that for cost minimization. For HTL pathway, the selected biomass supply counties are increased from 49 counties under cost minimization to 71 counties under GHG minimization.

The cost and GHG optimization results vary in unit production costs and GHG emissions for all three pathways (Table 7). HTL requires the lowest production costs but provide the highest GHG emissions under the economic and environmental optimizations. FT provides the lowest GHG emissions but requires a relatively high production cost. ATJ requires the highest production costs under both cost and GHG optimization scenarios. The range of cost and GHG emissions vary for three pathways. FT yields a range from 0.10 to 0.76 kg CO₂/gal; whereas ATJ and HTL generate the GHG emissions above 2.48 kg CO₂/gal. HTL has a relatively narrow range of GHG emissions, increasing from 3.42 to 3.65 kg CO₂/gal; whereas FT and ATJ have a wide range of GHG emissions. Decreased GHG emissions would always lead to an increase of production costs. A sustainability performance among three pathways should be evaluated by considering the trade-off between production costs and GHG emissions.

4.4. Sustainability evaluation by Pareto-optimal curve analysis

The Pareto-optimal curves are provided by solving the optimization model at 20 constraint levels of GHG emissions for each pathway (Fig. 8). FT is most environmentally friendly while HTL yields lowest production cost among three conversion pathways. The results demonstrate that total production costs increase rapidly with the stricter

constraints of GHG emissions, but they remain relatively stable under the high GHG emission levels. The breakdown of costs varies in different scenarios for three conversion pathways (Fig. 8). The biorefinery related costs decrease with relaxed GHG emission constraints, while the biomass procurement and CSP related cost remain stable. This is because at the low GHG emission level, the system tends to choose counties with low GHG emissions of biomass production. This would lead to a distributed supply chain configuration with many locally operated CSPs and biorefineries. The system would not benefit from the economies of scale and lead to the increased total production costs. A centralized supply chain system has relatively low production costs but high GHG emissions (Fig. 8).

HTL shows the largest demand of supply counties, CSP and biorefinery facilities among three technologies due to its lower RJF conversion rate (Fig. 9). When minimal GHG emissions are allowed, the supply chain configurations tend to select a large number of supply counties with low biomass GHG emissions, so there is an increased the number of supply chain configurations (Fig. 9). For example, the number of biorefinery facilities increases from 2 to 16, 1 to 11, and 6 to 26 for ATJ, FT, and HTL, respectively. On the contrary, in order to achieve low production cost, the supply chain configurations select large biorefinery facilities for economies of scale.

To compare GHG emissions and production costs of the three conversion pathways with fossil jet fuel, we normalize the GHG emissions for all three RJF pathways by providing the credits for the savings of GHG emissions. All three pathways have a much lower GHG emissions than current jet fuel production at 11.67 kg CO₂/gal, but require a higher production costs [25]. We monetize the GHG emission credits to a level of 11.67 kg CO₂/gal, using the social cost of \$0.22 per kg CO₂ [47], and calculate the equivalent production costs for each scenario. Take the lowest cost scenario of FT for example, it requires a production cost of \$5.23/gal while emits 0.76 kg CO₂ per gallon. The credit value for FT is therefore \$2.40/gal. The equivalent production costs of FT would be \$2.83/gal after considering the credit of GHG emission savings. The results show that ATJ requires higher equivalent production costs than most scenarios of FT and HTL (Fig. 10). FT yields lowest equivalent production costs (\$2.83/gal) among all scenarios after considering the GHG emission credit. The equivalent production costs of HTL are slightly higher than FT, but it requires the much higher total investments as a result of its low jet fuel conversion rate. The increased demand of biomass would require a more complex supply chain configuration (Fig. 9), which increases the complexity of operations management. Therefore, we suggest FT pathway as a promising sustainable pathway due to its low GHG emissions with low production costs (Fig. 10).

The costs of the three RJF production approaches require at least \$4.64/gal (Table 7), much higher than that of fossil jet fuel at \$1.93/gal. RJF productions are not cost competitive after considering the credits of GHG emissions at the credit of \$0.22 per kg CO₂ (Fig. 10). The lowest production cost scenario by FT would be cost competitive to the fossil fuel production if it can receive the credit at \$0.30 per kg CO₂. The existing analysis of production costs and GHG emissions are based on the MASBI region with corn stover as feedstock. Further improvements should be considered to improve the conversion efficiency, reduce the biomass costs by considering multiple feedstocks. The developed optimization model is currently limited to supply chain optimization for single conversion pathway and single biomass feedstock. It is possible that an optimal renewable jet fuel supply chain system would consist of multiple conversion pathways with multiple biomass feedstocks. Further modeling improvements should incorporate the optimization of the combination of multiple biomass feedstocks and conversion pathways.

5. Conclusion

The development of renewable jet fuel (RJF) production requires systems analysis for both economic and environmental performance.

We developed a four-stage biomass-based supply chain optimization model to incorporate spatial, agricultural, techno-economical, and environmental data for multi-objective systems optimization. We applied the model in the Midwestern U.S. region to evaluate the sustainability performance of three RJF conversion pathways including alcohol-to-jet (ATJ), Fischer-Tropsch (FT), and hydrothermal liquefaction (HTL). HTL yields the lowest cost at \$4.64/gal, whereas FT is the most environmental-friendly with an emission of 0.10 kg CO₂/gal. Biorefinery related costs account for the majority of the total production costs; whereas biomass production and biorefinery GHG emissions are the main contributors for total GHG emissions. For all three pathways, the cost optimization analysis suggests a centralized supply chain configuration with large facilities; whereas the environmental optimization prefers a distributed system with many CSP and biorefinery facilities.

The Pareto-optimal curves demonstrate that production costs increase rapidly under low levels of GHG emissions for three conversion pathways. This indicates that the economic performance is sensitive to the constraint of GHG emissions. Considering the carbon price at \$0.22 per kg of CO₂ reduction, FT yields the lowest costs of \$2.83/gal, compared to HTL (\$2.86/gal) and ATJ (\$4.55/gal). It is not cost competitive to fossil fuel (\$1.93/gal) until the carbon price increases to \$0.30 per kg of CO₂ reduction.

Acknowledgments

This work was partially funded by the China National Key Research and Development Plan under Grant Number 2017YFD0700605 and Zhejiang University.

Appendix A. Supplementary data

Supplementary data to this article can be found online at <https://doi.org/10.1016/j.rser.2019.109403>.

References

- [1] Aviation Transport Action Group. Beginner's guide to aviation biofuels. <http://www.safug.org/assets/docs/beginners-guide-to-aviation-biofuels.pdf>; 2011, Accessed date: August 2017.
- [2] Aviation Transport Action Group. Aviation benefits beyond borders. http://aviationbenefits.org/media/26786/ATAG_AviationBenefits2014_FULL_LowRes.pdf; 2014, Accessed date: August 2017.
- [3] Awudu I, Zhang J. Uncertainties and sustainability concepts in biofuel supply chain management: a review. *Renew Sustain Energy Rev* 2012;16(2):1359–68.
- [4] Biocombustibles ASA. <http://biocombustibles.asa.gob.mx/>; 2015, Accessed date: 14 October 2016.
- [5] Gutiérrez-Antonio C, Gómez-Castro FI, de Lira-Flores JA, Hernández S. A review on the production processes of renewable jet fuel. *Renew Sustain Energy Rev* 2017;79:709–29.
- [6] Wei H, Liu W, Chen X, Yang Q, Li J, Chen H. Renewable bio-jet fuel production for aviation: a review. *Fuel* 2019;254:115599.
- [7] Yang J, Xin Z, Corscadden K, Niu H. An overview on performance characteristics of bio-jet fuels. *Fuel* 2019;237:916–36.
- [8] Staples MD, Malina R, Olcay H, Pearson MN, Hileman JI, Boies A. Lifecycle greenhouse gas footprint and minimum selling price of renewable diesel and jet fuel from fermentation and advanced fermentation production technologies. *Energy Environ Sci* 2014;7(5):1545–54.
- [9] Hileman JI, Stratton RW. Alternative jet fuel feasibility. *Transp Policy* 2014;34:52–62.
- [10] Mirkouei A, Haapala KR, Sessions J, Murthy GS. A review and future directions in techno-economic modeling and optimization of upstream forest biomass to bio-oil supply chains. *Renew Sustain Energy Rev* 2017;67:15–35.
- [11] Staples MD, Malina R, Barrett SRH. The limits of bioenergy for mitigating global life-cycle greenhouse gas emissions from fossil fuels. *Nat Energy* 2017;2(2):16202.
- [12] Han J, Tao L, Wang M. Well-to-wake analysis of ethanol-to-jet and sugar-to-jet pathways. *Biotechnol Biofuels* 2017;10(1):21.
- [13] Sepehri A, Sarrafzadeh MH. Activity enhancement of ammonia-oxidizing bacteria and nitrite-oxidizing bacteria in activated sludge process: metabolite reduction and CO₂ mitigation intensification process. *Appl Water Sci* 2019;9(5):131.
- [14] de Jong S, Hoefnagels R, Faaij A, Slade R, Mawhood R, Junginger M. The feasibility of short-term production strategies for renewable jet fuels – a comprehensive techno-economic comparison. *Biofuels Bioprod Bioref* 2015;9:778–800.
- [15] Mawhood R, Gazis E, De Jong S, Hoefnagels R, Slade R. Production pathways for renewable jet fuel: a review of commercialization status and future prospects. *Biofuels Bioprod Bioref* 2016;10(4):462–84.

- [16] Mawhood R, Cobas AR, Slade R. Establishing a European renewable jet fuel supply chain: the technoeconomic potential of biomass conversion technologies. 2014<http://www.climate-kic.org/projects/renewable-jet-fuel-supply-chain-development-and-flight-operations> accessed March, 2016.
- [17] Wang WC. Techno-economic analysis of a bio-refinery process for producing Hydro-processed Renewable Jet fuel from Jatropha. *Renew Energy* 2016;95:63–73.
- [18] Natelson RH, Wang WC, Roberts WL, Zering KD. Technoeconomic analysis of jet fuel production from hydrolysis, decarboxylation, and reforming of camelina oil. *Biomass Bioenergy* 2015;75:23–34.
- [19] Pearson M, Wollersheim C, Hileman J. A techno-economic review of hydro-processed renewable esters and fatty acids for jet fuel production. *Biofuels Bioprod Bioref* 2013;7(1):89–96.
- [20] Pham V, Holtzapfel M, El-Halwagi M. Techno-economic analysis of biomass to fuel conversion via the MixAlco process. *J Ind Microbiol Biotechnol* 2010;37(11):1157–68.
- [21] Bwapwa JK, Anandraj A, Trois C. Possibilities for conversion of microalgae oil into aviation fuel: a review. *Renew Sustain Energy Rev* 2017;80:1345–54.
- [22] Scaldaferrri CA, Pasa VMD. Green diesel production from upgrading of cashew nut shell liquid. *Renew Sustain Energy Rev* 2019;111:303–13.
- [23] Reimer JJ, Zheng X. Economic analysis of an aviation bioenergy supply chain. *Renew Sustain Energy Rev* 2017;77:945–54.
- [24] Agusdinata DB, Zhao F, Ileleji K, DeLaurentis D. Life cycle assessment of potential biojet fuel production in the United States. *Environ Sci Technol* 2011;45(21):9133–43.
- [25] de Jong S, Antonissen K, Hoefnagels R, Lonza L, Wang M, Faaij A, et al. Life-cycle analysis of greenhouse gas emissions from renewable jet fuel production. *Biotechnol Biofuels* 2017;10(1):64.
- [26] Michailos S. Process design, economic evaluation and life cycle assessment of jet fuel production from sugar cane residue. *Environ Prog Sustain Energy* 2018;37(3):1227–35.
- [27] Yang Y, Brammer JG, Wright DG, Scott JA, Serrano C, Bridgwater AV. Combined heat and power from the intermediate pyrolysis of biomass materials: performance, economics and environmental impact. *Appl Energy* 2017;191:639–52.
- [28] Seber G, Malina R, Pearson MN, Olcay H, Hileman JI, Barrett SR. Environmental and economic assessment of producing hydroprocessed jet and diesel fuel from waste oils and tallow. *Biomass Bioenergy* 2014;67:108–18.
- [29] Malladi KT, Sowlati T. Biomass logistics: a review of important features, optimization modeling and the new trends. *Renew Sustain Energy Rev* 2018;94:587–99.
- [30] Pérez ATE, Camargo M, Rincón PCN, Marchant MA. Key challenges and requirements for sustainable and industrialized biorefinery supply chain design and management: a bibliographic analysis. *Renew Sustain Energy Rev* 2017;69:350–9.
- [31] Lin T, Rodríguez LF, Davis S, Khanna M, Shastri Y, Grift T, et al. Biomass feedstock preprocessing and long-distance transportation logistics. *Glob Chang Biol Bioenergy* 2016;8(1):160–70.
- [32] Castillo-Villar KK. Metaheuristic algorithms applied to bioenergy supply chain problems: theory, review, challenges, and future. *Energies* 2014;7(11):7640–72.
- [33] Ekşioğlu Sandra D, Acharya A, Leightley LE, Arora S. Analyzing the design and management of biomass-to-biorefinery supply chain. *Comput Ind Eng* 2009;57(4):1342–52.
- [34] Roni MS, Thompson DN, Hartley DS. Distributed biomass supply chain cost optimization to evaluate multiple feedstocks for a biorefinery. *Appl Energy* 2019;254:113660.
- [35] Malladi KT, Sowlati T. Biomass logistics: a review of important features, optimization modeling and the new trends. *Renew Sustain Energy Rev* 2018;94:587–99.
- [36] Nugroho YK, Zhu L. Platforms planning and process optimization for biofuels supply chain. *Renew Energy* 2019;140:563–79.
- [37] Niziolek AM, Onel O, Tian Y, Floudas CA, Pistikopoulos EN. Municipal solid waste to liquid transportation fuels—part iii: an optimization-based nationwide supply chain management framework. *Comput Chem Eng* 2018;116:468–87.
- [38] Lin T, Rodríguez LF, Shastri YN, Hansen AC, Ting K. GIS-enabled biomass ethanol supply chain optimization: model development and Miscanthus application. *Biofuels Bioprod Bioref* 2013;7(3):314–33.
- [39] Kumar A, Cameron JB, Flynn PC. Pipeline transport and simultaneous saccharification of corn stover. *Bioresour Technol* 2005;96(7):819–29.
- [40] Leila M, Whalen J, Bergthorson J. Strategic spatial and temporal design of renewable diesel and biojet fuel supply chains: case study of California, USA. *Energy* 2018;156:181–95.
- [41] Tong K, You F, Rong G. Robust design and operations of hydrocarbon biofuel supply chain integrating with existing petroleum refineries considering unit cost objective. *Comput Chem Eng* 2014;68:128–39.
- [42] Elia JA, Baliban RC, Floudas CA, Gurau B, Weingarten MB, Klotz SD. Hardwood biomass to gasoline, diesel, and jet fuel: 2. Supply chain optimization framework for a network of thermochemical refineries. *Energy Fuels* 2013;27(8):4325–52.
- [43] Eranki PL, Manowitz DH, Bals BD, Izaurralde RC, Kim S, Dale BE. The watershed-scale optimized and rearranged landscape design (WORLD) model and local biomass processing depots for sustainable biofuel production: integrated life cycle assessments. *Biofuels Bioprod Bioref* 2013;7(5):537–50.
- [44] Cobuloglu HI. A mixed-integer optimization model for the economic and environmental analysis of biomass production. *Biomass Bioenergy* 2014;67(5):8–23.
- [45] Yue D, Kim MA, You F. Design of sustainable product systems and supply chains with life cycle optimization based on functional unit: general modeling framework, mixed-integer nonlinear programming algorithms and case study on hydrocarbon biofuels. *ACS Sustainable Chem Eng* 2013;1(8):1003–14.
- [46] You F, Wang B. Life cycle optimization of biomass-to-liquid supply chains with distributed–centralized processing networks. *Ind Eng Chem Res* 2011;50(17):10102–27.
- [47] Moore FC, Diaz DB. Temperature impacts on economic growth warrant stringent mitigation policy. *Nat Clim Chang* 2015;5(2):127.
- [48] Argonne National Laboratory. Greenhouse Gases, Regulated Emissions, and Energy Use in Transportation (GREET) GREET.net Computer Model 2015. Argonne, IL: Argonne National Laboratory; 2015 Available at: <https://greet.es.anl.gov>, Accessed date: January 2017.
- [49] Argonne National Laboratory. Greenhouse Gases, Regulated Emissions, and Energy Use in Transportation (GREET) GREET_1_2015 Excel model 2015. Argonne, IL: Argonne National Laboratory; 2015 <https://greet.es.anl.gov>, Accessed date: January 2017.
- [50] Tews LJ, Zhu Y, Drennan C, Elliott DC, Snowden-Swan LJ, Onarheim K, et al. Biomass Direct Liquefaction Options. Technoeconomic and Life Cycle Assessment. Richland, WA (United States): Pacific Northwest National Lab.(PNNL); 2014.
- [51] Ereev SY, Patel MK. Standardized cost estimation for new technology (SCENT)-methodology and tool. *J Bus Chem* 2012;31–48.
- [52] Wyman O. Policy working group. <https://psu.box.com/s/dmu1zym61wzpye2trdm5xtiefyc8oa05>; 2013, Accessed date: June 2017.
- [53] USDA Farm Service Agency. Acreage data as of August 1 2015 <https://www.fsa.usda.gov/news-room/efoia/electronic-reading-room/frequently-requested-information/crop-acreage-data/index>; 2015, Accessed date: March 2017.
- [54] Mani S, Tabil LG, Sokhansanj S. Specific energy requirement for compacting corn stover. *Bioresour Technol* 2006;97(12):1420–6.